Exploring shell structure of nuclides in proximity of doubly-magic ^{132}Sn

Angela Gargano, INFN Napoli

Why ^{132}Sn region?

The only region around a heavy, neutron rich doubly-closed shell nucleus far-off stability experimentally accessible today

➢ gives important information, from the nuclear structure point of view, on the shell evolution and the underlying driving forces

➢ is of great relevance (especially nuclei with Z<50) for the description of the rapid neutron capture process of nucleosynthesis

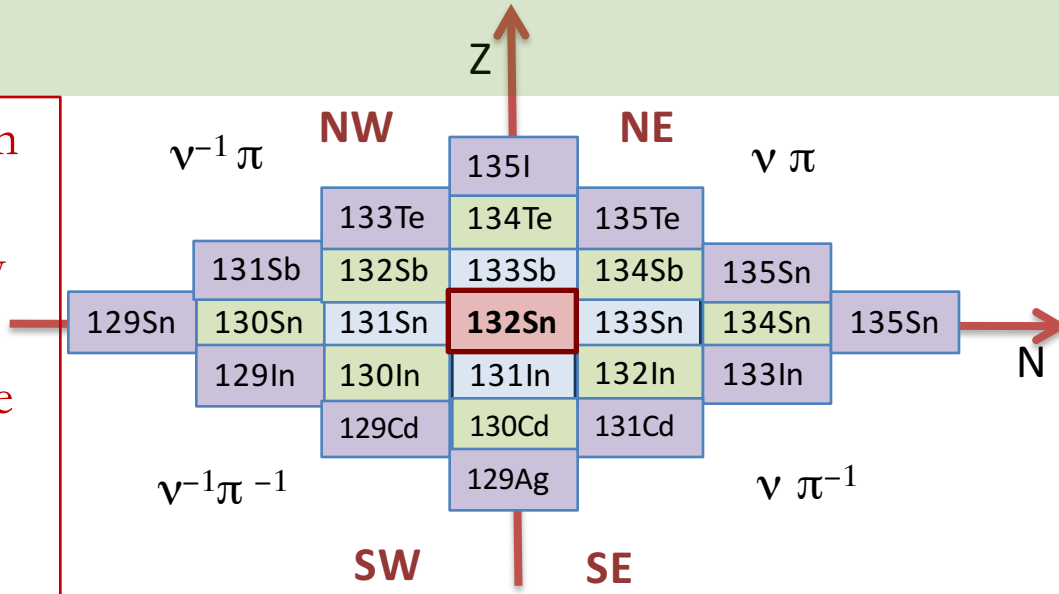

Why ^{132}Sn region?

The only region around a heavy, neutron-rich doubly-closed shell nucleus far-off stability experimentally accessible today

➢ gives important information, from the nuclear structure point of view, on the shell evolution and the underlying driving forces

➢ is of great relevance (especially nuclei with Z<50) for the description of the rapid neutron capture process of nucleosynthesis

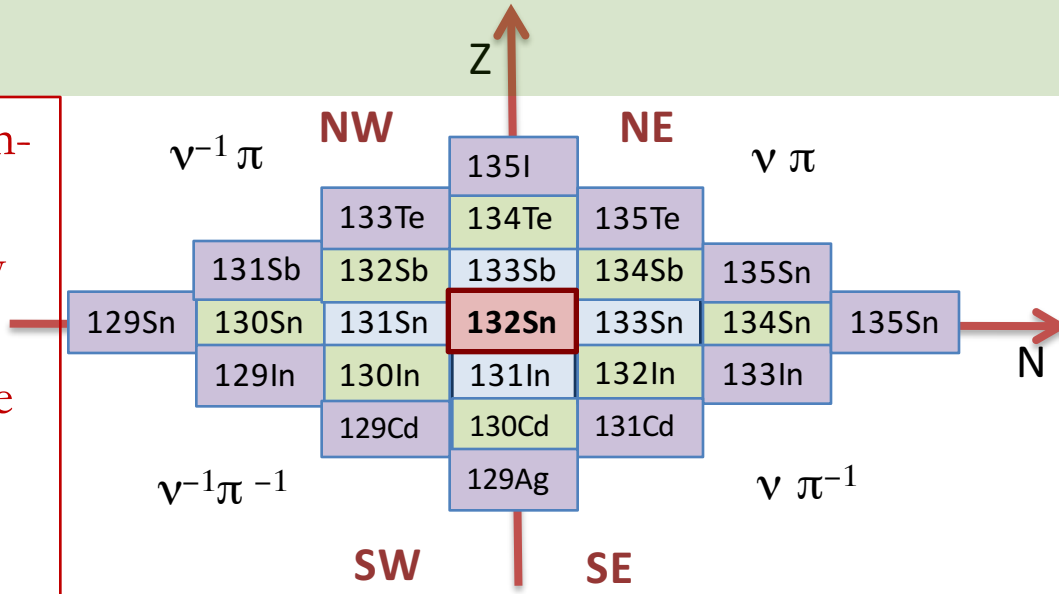

Experimental information → allows us to test nuclear models
(for shell model: single-particle energies, two-body matrix elements of the residual interaction and effective electromagnetic operators) **and to ascertain their capability to provide reliable predictions for nuclei**

✓ **which are still unaccessible for present experiments**

✓ **involved in 0ν2β decay (^{130}Te, ^{136}Xe)**

The "realistic" Shell Model

$$H_{\text{eff}}\psi_\alpha = H_0 + V_{\text{eff}}\psi_\alpha = E_\alpha\psi_\alpha \quad \text{with } H_0 = T + U$$

in the model space for only valence nucleons

The "realistic" Shell Model

$$H_{\text{eff}}\psi_\alpha = H_0 + V_{\text{eff}}\psi_\alpha = E_\alpha\psi_\alpha \quad \text{with } H_0 = T + U$$

in the model space for only valence nucleons

$$V_{NN}\ (+V_{NNN}) \Rightarrow \text{many-body theory} \Rightarrow H_{\text{eff}}$$

Definition [for 2 valence-nucleon systems]

The eigenvalues of H_{eff} belong to the set of eigenvalues of the full nuclear hamiltonian in the full Hilbert space

The "realistic" Shell Model

$$H_{\text{eff}}\psi_\alpha = H_0 + V_{\text{eff}}\psi_\alpha = E_\alpha\psi_\alpha \quad \text{with } H_0 = T + U$$

in the model space for only valence nucleons

$$V_{NN}\ (+V_{NNN}) \Rightarrow \text{many-body theory} \Rightarrow H_{\text{eff}}$$

Definition [for 2 valence-nucleon systems]

The eigenvalues of H_{eff} belong to the set of eigenvalues of the full nuclear hamiltonian in the full Hilbert space

H_{eff} takes into account in an effective way all the degrees of freedom not considered explicitly: namely core nucleons and excitations of valence nucleons into the shells above the model space

Flow chart of a RSMC

- Choice of the free *NN* potential
- Choice of the model space better tailored to study the system under investigation
- Derivation of the effective Hamiltonian making use of many-body theory
- Diagonalization of the Hamiltonian matrix & calculations of physical observables as energies, electromagnetic transition probabilities*, …

*Need to use microscopic effective operators consistent with the effective Hamiltonian

1st step: choice of the NN potential

Several realistic potentials $\chi^2/datum \simeq 1$:
CD-Bonn, Argonne V18, Nijmegen, ...

or derived by the chiral effective field theory

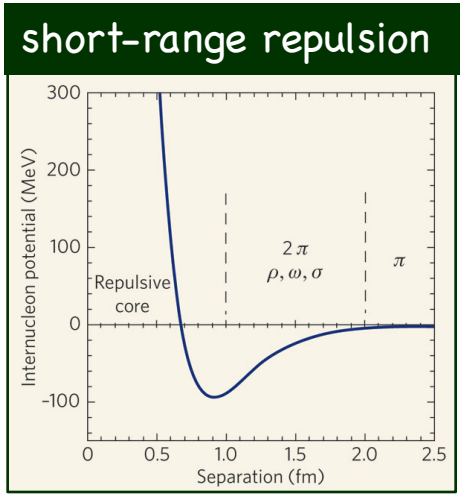

1st step: choice of the NN potential

Several realistic potentials $\chi^2/datum \simeq 1$:
CD-Bonn, Argonne V18, Nijmegen, ...

or derived by the chiral effective field theory

- normalization procedure for V_{NN}

short-range repulsion

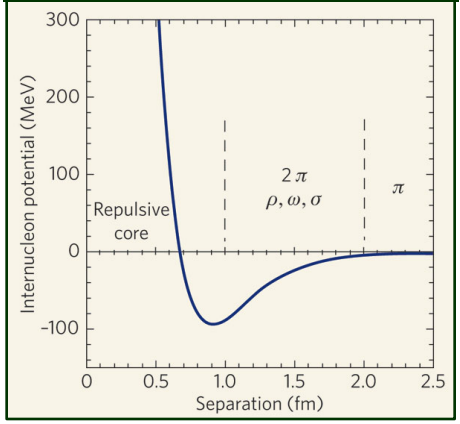

- **low momentum potentials:**

✓ **$V_{low\text{-}k}$**

preserves the properties of the original NN potential up to a momentum-space cutoff Λ

✓ **chiral potentials defined for momenta below a low cutoff**

2nd step: choice of the model space

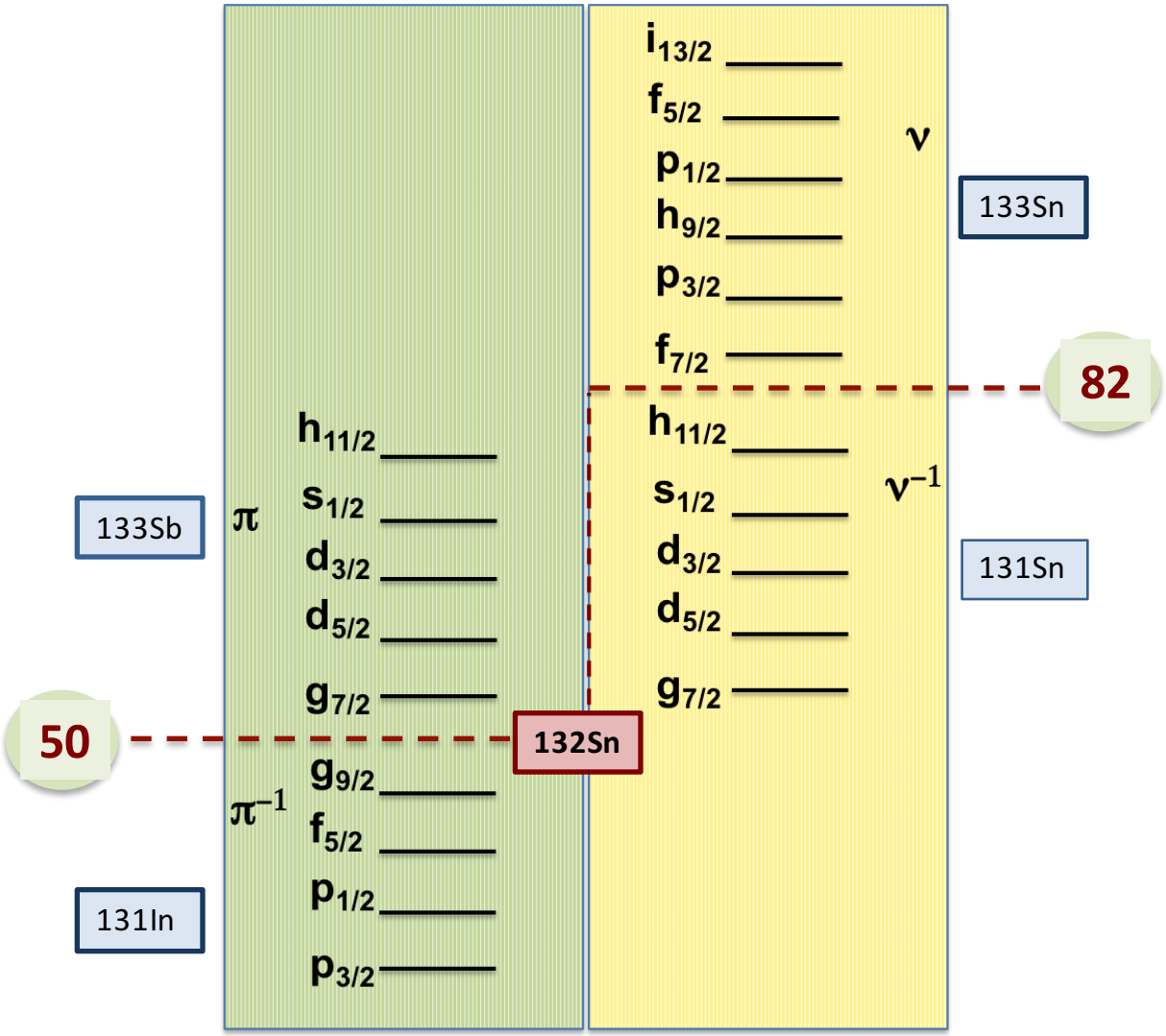

3rd step: derivation of the effective interaction by the folded diagram method

H_{eff} is written as a series in terms of the $\hat{Q}$ - box and its derivatives.

For instance

$$H^{\text{eff}} = \sum_{i=0}^{\infty} F_i,$$

where

$$F_0 = \hat{Q}(\epsilon_0)$$
$$F_1 = \hat{Q}_1(\epsilon_0)\hat{Q}(\epsilon_0)$$
$$F_2 = \hat{Q}_2(\epsilon_0)\hat{Q}(\epsilon_0)\hat{Q}(\epsilon_0) + \hat{Q}_1(\epsilon_0)\hat{Q}_1(\epsilon_0)\hat{Q}(\epsilon_0)$$
$$\ldots.$$

$$\hat{Q}(\epsilon) = PH_1P + PH_1Q\frac{1}{\epsilon - QHQ}QH_1P.$$

where $H_1 = V_{low\text{-}k} - U$; P= model space; $Q = 1 - P$; $\varepsilon = PH_0P$;

3rd step: derivation of the effective interaction by the folded diagram method

H_{eff} is written as a series in terms of the $\hat{Q}$ - box and its derivatives.

For instance

$$H^{\text{eff}} = \sum_{i=0}^{\infty} F_i,$$

where

$$F_0 = \hat{Q}(\epsilon_0)$$
$$F_1 = \hat{Q}_1(\epsilon_0)\hat{Q}(\epsilon_0)$$
$$F_2 = \hat{Q}_2(\epsilon_0)\hat{Q}(\epsilon_0)\hat{Q}(\epsilon_0) + \hat{Q}_1(\epsilon_0)\hat{Q}_1(\epsilon_0)\hat{Q}(\epsilon_0)$$
$$\ldots.$$

$$\hat{Q}(\epsilon) = PH_1P + PH_1Q\frac{1}{\epsilon - QHQ}QH_1P.$$

where $H_1 = V_{low\text{-}k} - U$; P= model space; $Q = 1 - P$; $\varepsilon = PH_0P$;

The series is summed by iterative techniques
(Krenciglowa-Kuo, Lee-Suzuki)

Perturbative calculation

The diagrammatic expansion of the $\hat{Q}$-box

1-body diagrams up to 2nd order **S-box**

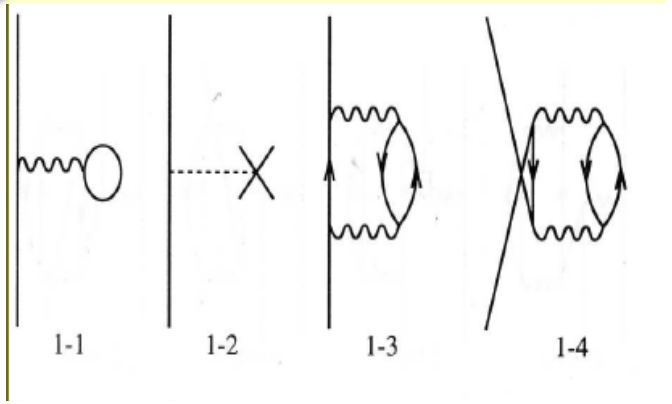

2-body diagrams up to 2nd order:

V **V_{1p1h}** **V_{2p}** **V_{2p2h}**

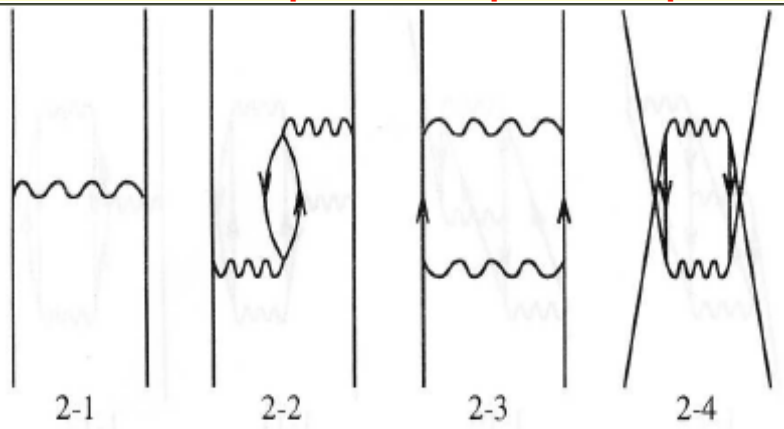

Perturbative calculation

The diagrammatic expansion of the $\hat{Q}$-box

1-body diagrams up to 2nd order **S-box**

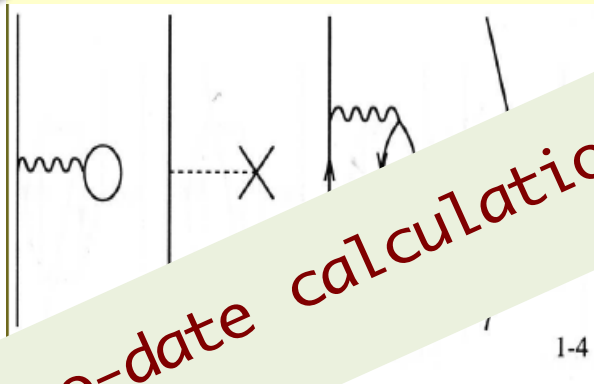

2-body diagrams V V

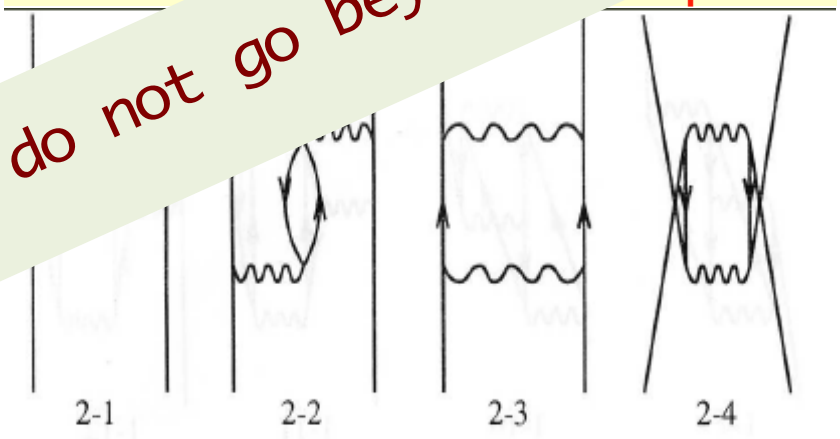

up-to-date calculations do not go beyond third order!

Results in ^{132}Sn region

CD-Bonn

$V_{\text{low-k}}$

(Λ=2.2 fm^{-1}) + Coulomb interaction

V_{eff} @ second order

Model space: one major shell for protons/neutrons

with SP energies from experiment

Realistic shell-model studies around ^{132}Sn

F. Andreozzi, L. Coraggio, A. Covello, A. Gargano, T.T.S. Kuo, and A. Porrino, *Structure of neutron-rich nuclei around ^{132}Sn*, Phys. Rev. C **56**, R16 (1997)

Energy spectra and electromagnetic propertis of nuclei below and above Z=50
Behavior of odd- even mass staggering around ^{132}Sn
Evolution of single-particle states beyond ^{132}Sn
Mixed-symmetry states
Predictions for exotic Sn isotopes with N>82
Proton-neutron multiplets
Similarity of nuclear structure in the ^{132}Sn and ^{208}Pb regions
Role of three-nucleon forces in neutron-rich nuclei beyond ^{132}Sn

satisfactory description of nuclear structure properties, although some problems still remain to be solved

Realistic shell-model studies around ^{132}Sn

F. Andreozzi, L. Coraggio, A. Covello, A. Gargano, T.T.S. Kuo, and A. Porrino, *Structure of neutron-rich nuclei around ^{132}Sn*, Phys. Rev. C **56**, R16 (1997)

Energy spectra and electromagnetic propertis of nuclei below and above Z=50
Behavior of odd- even mass staggering around ^{132}Sn
Evolution of single-particle states beyond ^{132}Sn
Mixed-symmetry states
Predictions for exotic Sn isotopes with N>82
Proton-neutron multiplets
Similarity of nuclear structure in the ^{132}Sn and ^{208}Pb regions
Role of three-nucleon forces in neutron-rich nuclei beyond ^{132}Sn

satisfactory description of nuclear structure properties, although some problems still remain to be solved

- **$1/2^+ \rightarrow 3/2^+$ M1 transition in ^{129}Sn**
- **$(\pi\, g_{9/2})^{-1} \otimes \nu\, f_{7/2}$ multiplet in ^{132}In**

- R. Lica, H. Mach, L. M. Fraile, A. Gargano *et al*, *Fast-timing study of the l-forbidden $1/2^+ \rightarrow 3/2^+$ M1 transition in ^{129}Sn*, Phys. Rev. C **93**, 044303 (2016)
- A. Jungclaus, A. Gargano *et al*, *First observation of γ rays emitted from excited states south-east of ^{132}Sn: The $\pi g_{9/2}^{-1} \otimes \nu f_{7/2}$ multiplet of $^{132}In_{83}$*, Phys. Rev. C **93**, 041301(R) (2016)

PHYSICAL REVIEW C **93**, 044303 (2016)

Fast-timing study of the l-forbidden $1/2^+ \rightarrow 3/2^+$ $M1$ transition in ^{129}Sn

β^- decay of ^{129}In isomers @ ISOLDE

PHYSICAL REVIEW C **93**, 044303 (2016)

Fast-timing study of the l-forbidden $1/2^+ \rightarrow 3/2^+$ $M1$ transition in ^{129}Sn

β^- decay of ^{129}In isomers @ ISOLDE

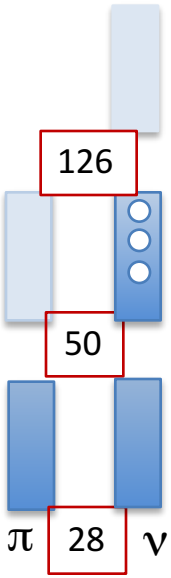

^{129}Sn ⟺ 3 neutron holes in the 50-82 shell

Fast-timing study of the *l*-forbidden $1/2^+ \rightarrow 3/2^+$ *M*1 transition in ^{129}Sn

β^- decay of ^{129}In isomers @ ISOLDE

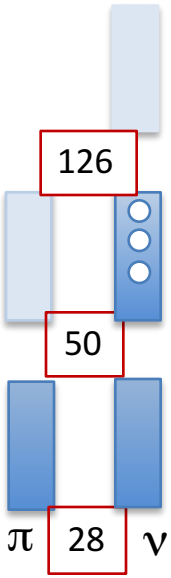

^{129}Sn ⟺ **3 neutron holes in the 50-82 shell**

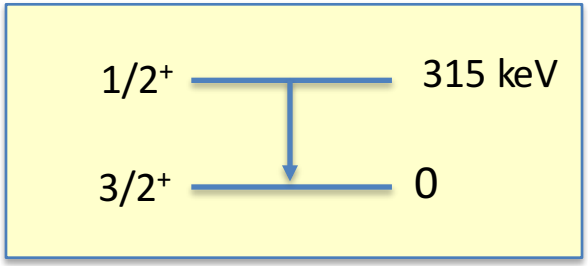

^{129}Sn	
$3/2^+$	$(1d_{1/2})^{-1}$
$1/2^+$	$(2s_{1/2})^{-1}$

→ **slow l forbidden (Δl=2) M1 transition**
E2 transition hindered

PHYSICAL REVIEW C **93**, 044303 (2016)

Fast-timing study of the *l*-forbidden $1/2^+ \rightarrow 3/2^+$ *M*1 transition in ^{129}Sn

β^- decay of ^{129}In isomers @ ISOLDE

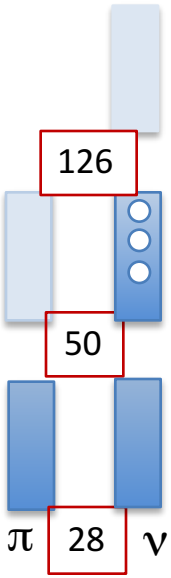

^{129}Sn ⟺ **3 neutron holes in the 50-82 shell**

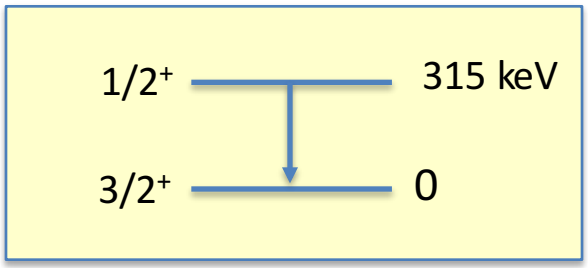

^{129}Sn	
$3/2^+$	$(1d_{1/2})^{-1}$
$1/2^+$	$(2s_{1/2})^{-1}$

→ **slow l forbidden (Δl=2) M1 transition**
E2 transition hindered

$1/2^+$ $T_{1/2}$= 19(10) ps → (assuming a pure M1 transition)
B(M1; $1/2^+ \rightarrow 3/2^+$)=6.4(30) × 10^{-2} μ_N^2

Relatively fast M1 transition

Fast-timing study of the *l*-forbidden $1/2^+ \rightarrow 3/2^+$ *M*1 transition in ^{129}Sn

E_{exc} (in keV)		
	Calc	Expt
$1/2^+$	294	315

Percentage of the wf configurations
$3/2^+ \rightarrow (1d_{3/2})^{-1}(nlj)^{-2}$ & $1/2^+ \rightarrow (2s_{1/2})^{-1}(nlj)^{-2}$

J^π	$(nl_j)^{-2}$				
	$(0h_{11/2})^{-2}$	$(1d_{3/2})^{-2}$	$(2s_{1/2})^{-2}$	$(1d_{5/2})^{-2}$	$(0g_{7/2})^{-2}$
$3/2^+$	69%	12%	8%	6%	5%
$1/2^+$	60%	27%	7%		5%

Fast-timing study of the *l*-forbidden $1/2^+ \rightarrow 3/2^+$ *M*1 transition in ^{129}Sn

E_{exc} (in keV)		
	Calc	Expt
$1/2^+$	294	315

Percentage of the wf configurations
$3/2^+ \rightarrow (1d_{3/2})^{-1}(nlj)^{-2}$ & $1/2^+ \rightarrow (2s_{1/2})^{-1}(nlj)^{-2}$

J^π	$(nl_j)^{-2}$				
	$(0h_{11/2})^{-2}$	$(1d_{3/2})^{-2}$	$(2s_{1/2})^{-2}$	$(1d_{5/2})^{-2}$	$(0g_{7/2})^{-2}$
$3/2^+$	69%	12%	8%	6%	5%
$1/2^+$	60%	27%	7%		5%

$$e^{\text{eff}} = 0.7e$$

$$g_l^{\text{free}} = 0,\ g_s = 0.7 g_s^{\text{free}} = -2.68$$

B(E2; $1/2^+ \rightarrow 3/2^+$)	B(M1; $1/2^+ \rightarrow 3/2^+$)
32.89 e^2 fm^4	0.58 x 10^{-4} μ_N^2

PHYSICAL REVIEW C **93**, 044303 (2016)

Fast-timing study of the *l*-forbidden $1/2^+ \rightarrow 3/2^+$ *M*1 transition in ^{129}Sn

E_{exc} (in keV)		
	Calc	Expt
$1/2^+$	294	315

Percentage of the wf configurations
$3/2^+ \rightarrow (1d_{3/2})^{-1}(nlj)^{-2}$ & $1/2^+ \rightarrow (2s_{1/2})^{-1}(nlj)^{-2}$

J^π	$(nl_j)^{-2}$				
	$(0h_{11/2})^{-2}$	$(1d_{3/2})^{-2}$	$(2s_{1/2})^{-2}$	$(1d_{5/2})^{-2}$	$(0g_{7/2})^{-2}$
$3/2^+$	69%	12%	8%	6%	5%
$1/2^+$	60%	27%	7%		5%

$$e^{\text{eff}} = 0.7e$$

$$g_l^{\text{free}} = 0,\ g_s = 0.7 g_s^{\text{free}} = -2.68$$

B(E2; $1/2^+ \rightarrow 3/2^+$)	B(M1; $1/2^+ \rightarrow 3/2^+$)
32.89 e^2 fm^4	0.58 x 10^{-4} μ_N^2

two order of magnitude larger than the experimental value
$T_{1/2}$= 19(10) ps

T(E2)	T(M1)	$T_{1/2}$
0.13 x10^9 s^{-1}	0.03 x 10^9 s^{-1}	4 ns

Fast-timing study of the *l*-forbidden $1/2^+ \rightarrow 3/2^+$ *M*1 transition in ^{129}Sn

M1 effective operator

with core excitations microscopically taken into account by means of many-body perturbation theory, consistently with the derivation of the effective two-body interaction

Perturbation expansion: some diagrams

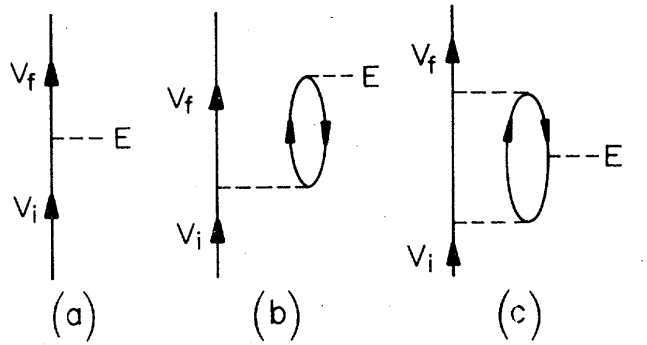

Fast-timing study of the l-forbidden $1/2^+ \rightarrow 3/2^+$ $M1$ transition in ^{129}Sn

M1 effective operator

with core excitations microscopically taken into account by means of many-body perturbation theory, consistently with the derivation of the effective two-body interaction

TABLE III. Comparison between the single-hole neutron $M1$ matrix elements (in μ_N) obtained using g factors $g_l^{\text{free}} = 0$, $g_s = -2.68$ (I), and those of the effective $M1$ operator (II) (see text for details).

a	b	$\langle a\|\|M1\|\|b\rangle_{(\text{I})}$	$\langle a\|\|M1\|\|b\rangle_{(\text{II})}$
$0g_{7/2}$	$0g_{7/2}$	1.65	1.36
$0g_{7/2}$	$1d_{5/2}$	0	0.15
$1d_{5/2}$	$1d_{5/2}$	− 1.92	− 1.89
$1d_{5/2}$	$1d_{3/2}$	2.05	1.88
$1d_{3/2}$	$1d_{3/2}$	1.02	1.05
$1d_{3/2}$	$2s_{1/2}$	0	0.10
$2s_{1/2}$	$2s_{1/2}$	− 1.62	− 1.61
$0h_{11/2}$	$0h_{11/2}$	− 2.49	− 2.48

Perturbation expansion: some diagrams

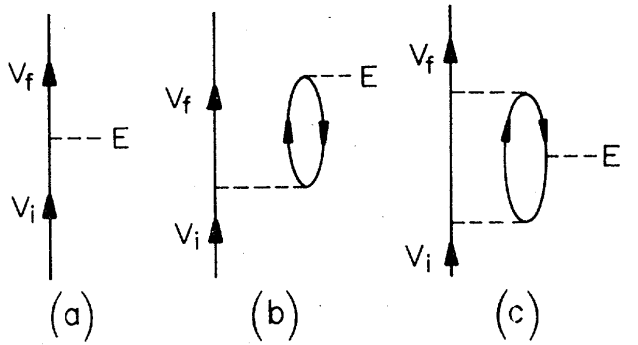

Fast-timing study of the *l*-forbidden $1/2^+ \rightarrow 3/2^+$ *M*1 transition in ^{129}Sn

M1 effective operator

with core excitations microscopically taken into account by means of many-body perturbation theory, consistently with the derivation of the effective two-body interaction

TABLE III. Comparison between the single-hole neutron $M1$ matrix elements (in μ_N) obtained using g factors $g_l^{\text{free}} = 0$, $g_s = -2.68$ (I), and those of the effective $M1$ operator (II) (see text for details).

a	b	$\langle a\|\|M1\|\|b\rangle_{(\mathrm{I})}$	$\langle a\|\|M1\|\|b\rangle_{(\mathrm{II})}$
$0g_{7/2}$	$0g_{7/2}$	1.65	1.36
$0g_{7/2}$	$1d_{5/2}$	0	0.15
$1d_{5/2}$	$1d_{5/2}$	− 1.92	− 1.89
$1d_{5/2}$	$1d_{3/2}$	2.05	1.88
$1d_{3/2}$	$1d_{3/2}$	1.02	1.05
$1d_{3/2}$	$2s_{1/2}$	0	0.10
$2s_{1/2}$	$2s_{1/2}$	− 1.62	− 1.61
$0h_{11/2}$	$0h_{11/2}$	− 2.49	− 2.48

Perturbation expansion: some diagrams

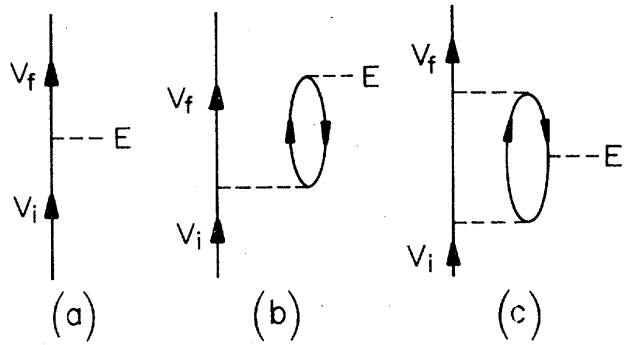

OBTD:

$(3)^{-1/2} \langle 3/2^+ || [a_{d3/2}{}^+ \otimes a_{s1/2}]^1 || 1/2^+ \rangle \sim 0.9$

Fast-timing study of the *l*-forbidden $1/2^+ \rightarrow 3/2^+$ *M*1 transition in ^{129}Sn

M1 effective operator

B(M1; $1/2^+ \rightarrow 3/2^+$)	T(M1)
$0.55 \times 10^{-2}\ \mu_N^2$	$3.42 \times 10^9\ s^{-1}$

$T_{1/2}$= 200 ps

20 times shorter than the $T_{1/2}$ obtained with empirical g factors and closer to the experimental value [19(10)ps]

Fast-timing study of the *l*-forbidden $1/2^+ \rightarrow 3/2^+$ *M*1 transition in ^{129}Sn

M1 effective operator

B(M1; $1/2^+ \rightarrow 3/2^+$)	T(M1)
0.55 x 10^{-2} μ_N^2	3.42 x 10^9 s^{-1}

$T_{1/2}$= 200 ps

➡ **20 times shorter than the $T_{1/2}$ obtained with empirical g factors and closer to the experimental value [19(10)ps]**

E2?

No substantial change is produced by using a microscopic effective E2 operator!
Effective charge for $\langle 1d_{3/2}||E2||2s_{1/2}\rangle$ ~0.8 ➤ an increase in T(E2) sligthly >1

PHYSICAL REVIEW C **93**, 044303 (2016)

Fast-timing study of the l-forbidden $1/2^+ \rightarrow 3/2^+$ $M1$ transition in ^{129}Sn

M1 effective operator

B(M1; $1/2^+ \rightarrow 3/2^+$)	T(M1)
$0.55 \times 10^{-2}\ \mu_N^2$	$3.42 \times 10^9\ s^{-1}$

$T_{1/2}$= 200 ps

➡ 20 times shorter than the $T_{1/2}$ obtained with empirical g factors and closer to the experimental value [19(10)ps]

E2?

No substantial change is produced by using a microscopic effective E2 operator!
Effective charge for $\langle 1d_{3/2}||E2||2s_{1/2}\rangle$ ~0.8 ➤ an increase in T(E2) sligthly >1

An enhancement of the T (E2) similar to the one obtained for the M1 transition would require a neutron effective charge equal to 10, a value without any physical meaning!!

→ **the $T_{1/2}(1/2^+)$ arises essentially from the M1 transition**

→ **the still existing difference between the experimental and calculated half-life may be from higher-order diagrams not included in the calculation of the M1 effective operator**

First observation of γ rays emitted from excited states south-east of ^{132}Sn: The $\pi g_{9/2}^{-1} \otimes \nu f_{7/2}$ multiplet of $^{132}In_{83}$

^{132}In ⟺ 1 proton hole in the 28-50 shell + 1 neutron particle in the 50 -82 shell

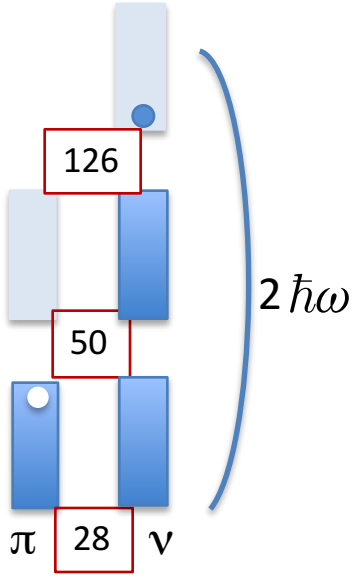

Identification of the first-excited states in ^{132}In SE of ^{132}Sn

$[(\pi\, g_{9/2})^{-1} \otimes \nu\, f_{7/2}]\ J^{\pi} = 1^{-} \ldots. 8^{-}$

PHYSICAL REVIEW C **93**, 041301(R) (2016)

First observation of γ rays emitted from excited states south-east of ^{132}Sn: The $\pi g_{9/2}^{-1} \otimes \nu f_{7/2}$ multiplet of $^{132}In_{83}$

^{132}In ⟺ 1 proton hole in the 28-50 shell + 1 neutron particle in the 50 -82 shell

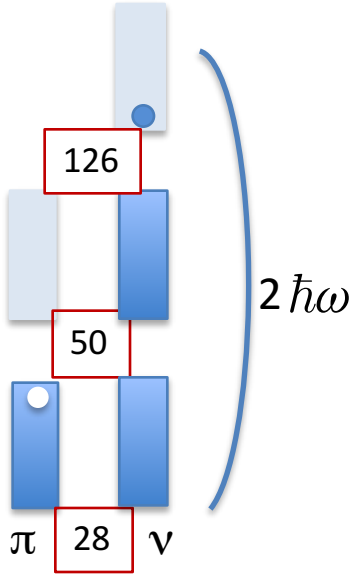

Identification of the first-excited states in ^{132}In SE of ^{132}Sn

$[(\pi\, g_{9/2})^{-1} \otimes \nu\, f_{7/2}]\ J^{\pi} = 1^{-} \ldots . 8^{-}$

Unique study case in the table of isotopes:

- the corresponding multiplets south-east of ^{78}Ni and ^{42}Si are currently not accessible for experimental studies

- the $(\pi 0h_{11/2})^{-1} \otimes \nu 1g_{9/2}$ multiplet in ^{208}Tl is distorted by the presence of the $2s_{1/2}$ and $1d_{3/2}$ proton orbitals

PHYSICAL REVIEW C **93**, 041301(R) (2016)

First observation of γ rays emitted from excited states south-east of ^{132}Sn: The $\pi g_{9/2}^{-1} \otimes \nu f_{7/2}$ multiplet of $^{132}In_{83}$

β-delayed neutron emission from ^{133}Cd @ RIBF of RIKEN

First observation of γ rays emitted from excited states south-east of ^{132}Sn: The $\pi g_{9/2}^{-1} \otimes \nu f_{7/2}$ multiplet of $^{132}In_{83}$

β-delayed neutron emission from ^{133}Cd @ RIBF of RIKEN

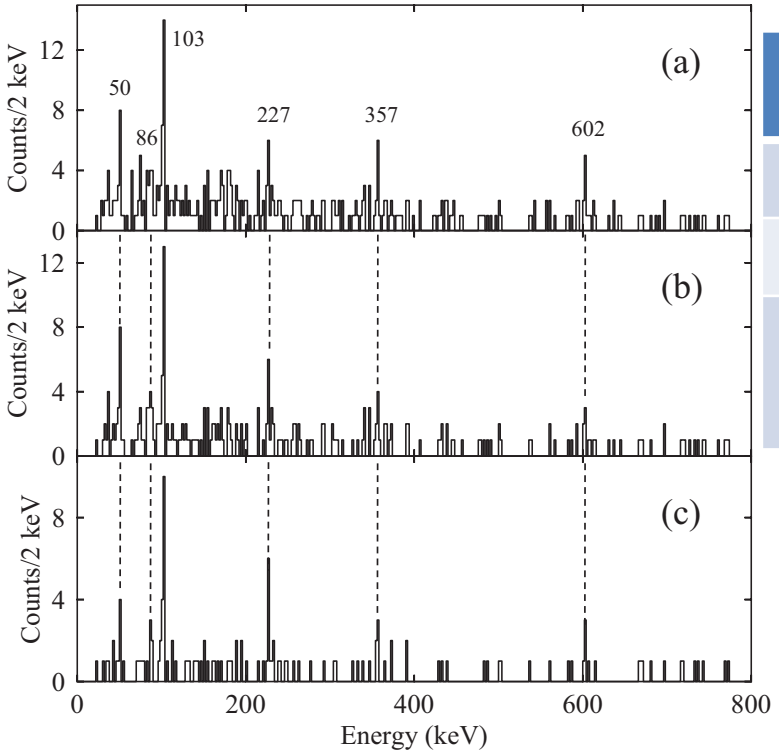

γ -ray spectra in prompt coincidence with decay events during the first 200 ms after the implantation of a ^{133}Cd ion	
a	Without further condition
b	requiring multiplicity one in the **γ -ray** detector
c	b +strict spatial correlation decay took place either in the Si detector in which the ion was implanted or in the one in front or behind

First observation of γ rays emitted from excited states south-east of ^{132}Sn: The $\pi g_{9/2}^{-1} \otimes \nu f_{7/2}$ multiplet of $^{132}In_{83}$

β-delayed neutron emission from ^{133}Cd @ RIBF of RIKEN

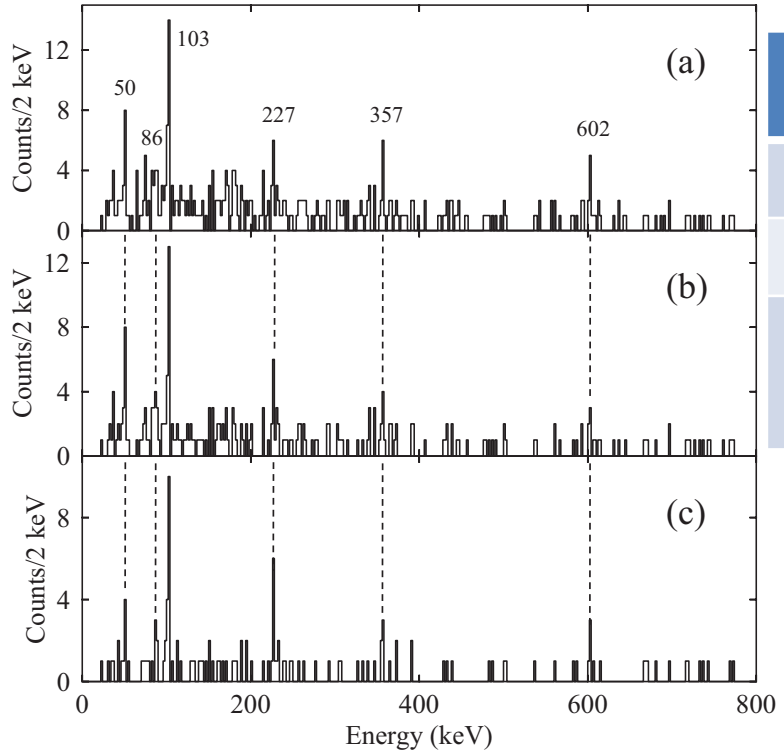

γ -ray spectra in prompt coincidence with decay events during the first 200 ms after the implantation of a ^{133}Cd ion	
a	Without further condition
b	requiring multiplicity one in the **γ -ray** detector
c	b +strict spatial correlation decay took place either in the Si detector in which the ion was implanted or in the one in front or behind

Six lines at energies of 50, 86, 103, 227, 357, 602 keV

PHYSICAL REVIEW C **93**, 041301(R) (2016)

First observation of γ rays emitted from excited states south-east of ^{132}Sn: The $\pi g_{9/2}^{-1} \otimes \nu f_{7/2}$ multiplet of $^{132}In_{83}$

β-delayed neutron emission from ^{133}Cd @ RIBF of RIKEN

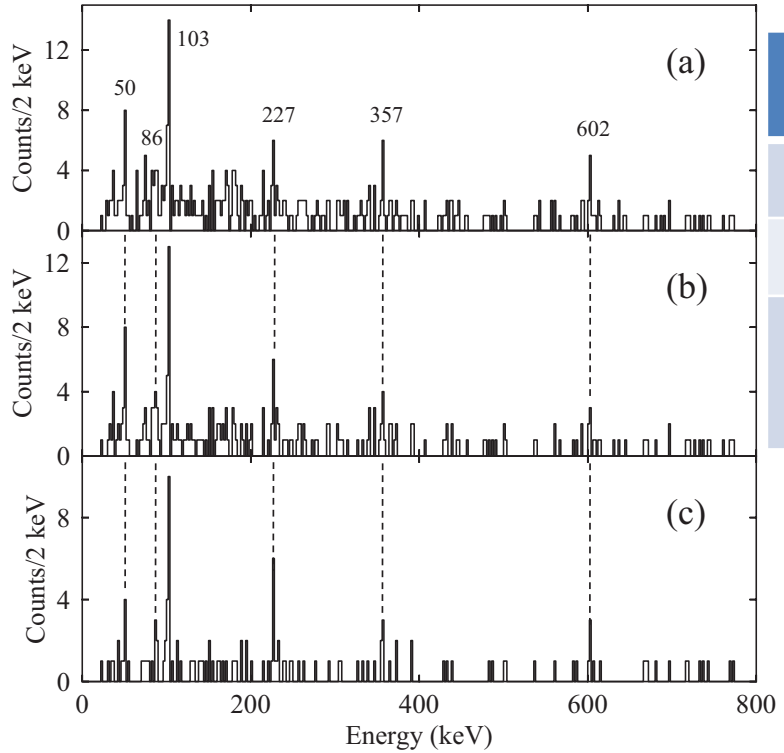

γ -ray spectra in prompt coincidence with decay events during the first 200 ms after the implantation of a ^{133}Cd ion	
a	Without further condition
b	requiring multiplicity one in the **γ -ray** detector
c	b +strict spatial correlation decay took place either in the Si detector in which the ion was implanted or in the one in front or behind

Six lines at energies of 50, 86, 103, 227, 357, 602 keV

The statistics accumulated are very limited so that no conclusive γγ coincidence information could be obtained

First observation of γ rays emitted from excited states south-east of ^{132}Sn: The $\pi g_{9/2}^{-1} \otimes \nu f_{7/2}$ multiplet of $^{132}In_{83}$

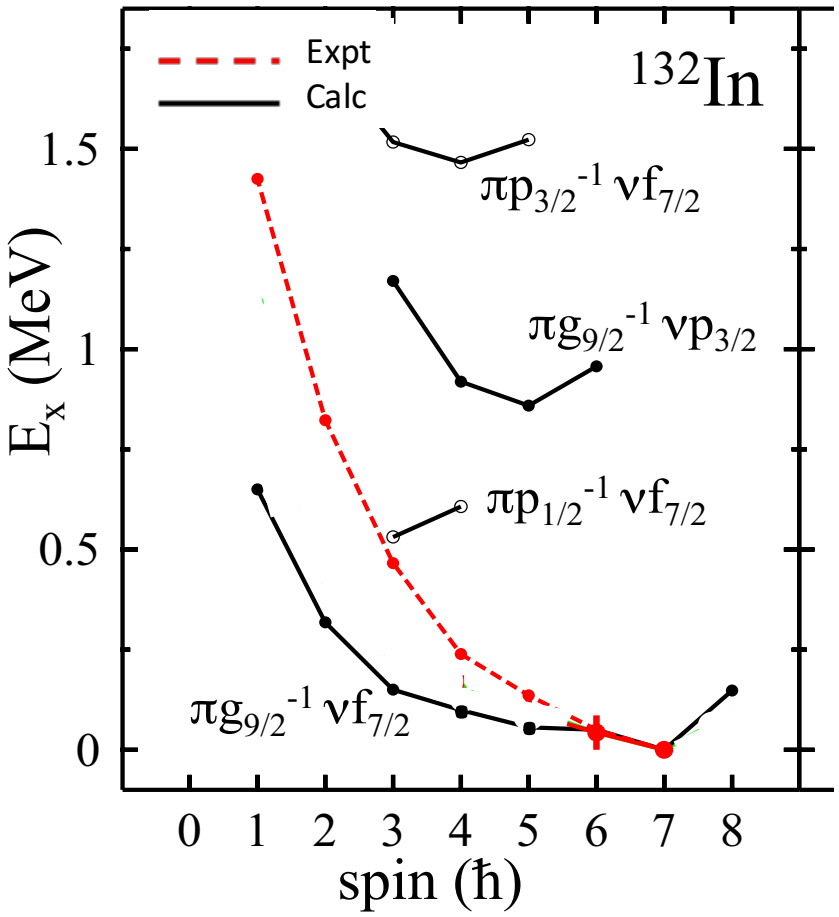

Assuming that the six observed γ rays correspond to the expected cascade of M1 transitions from the 1^- to the 7^- member of the $(\pi g_{9/2})^{-1} \otimes \nu f_{7/2}$ multiplet

The experimental energies are systematically higher than the calculated ones, leading to a total energy spread which is twice as large as theoretically predicted

average difference between experimental and calculated excitation energies is ~300 keV

First observation of γ rays emitted from excited states south-east of ^{132}Sn: The $\pi g_{9/2}^{-1} \otimes \nu f_{7/2}$ multiplet of $^{132}In_{83}$

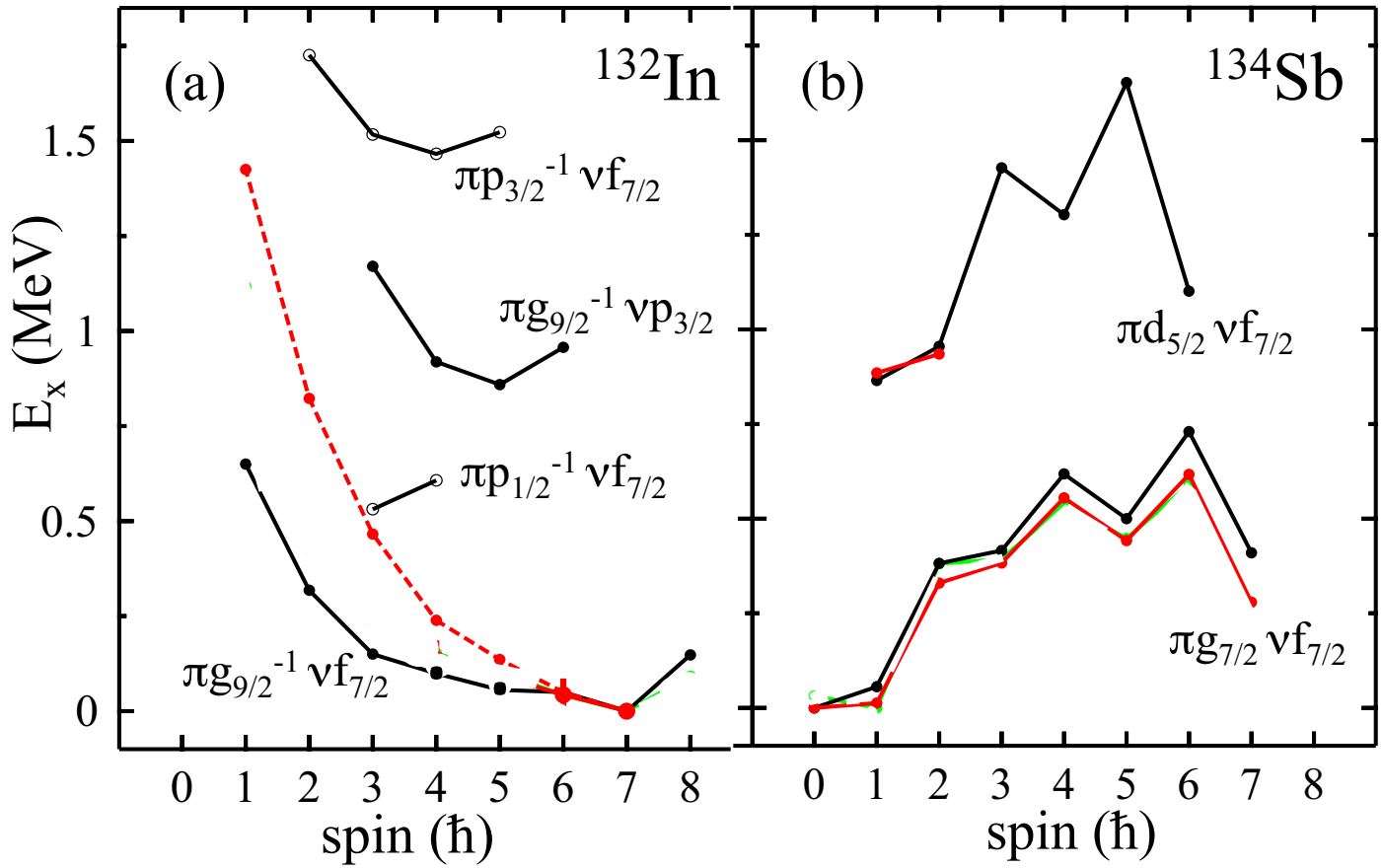

In ^{134}Sb, average difference between experimental and calculated level energies amounts to less than 10% of the SM energy spread

First observation of γ rays emitted from excited states south-east of ^{132}Sn: The $\pi g_{9/2}^{-1} \otimes \nu f_{7/2}$ multiplet of ^{132}In$_{83}$

Assuming that one of the lowest transitions within the multiplet is unobserved and adopting an energy of 25 ± 25 keV for this transition

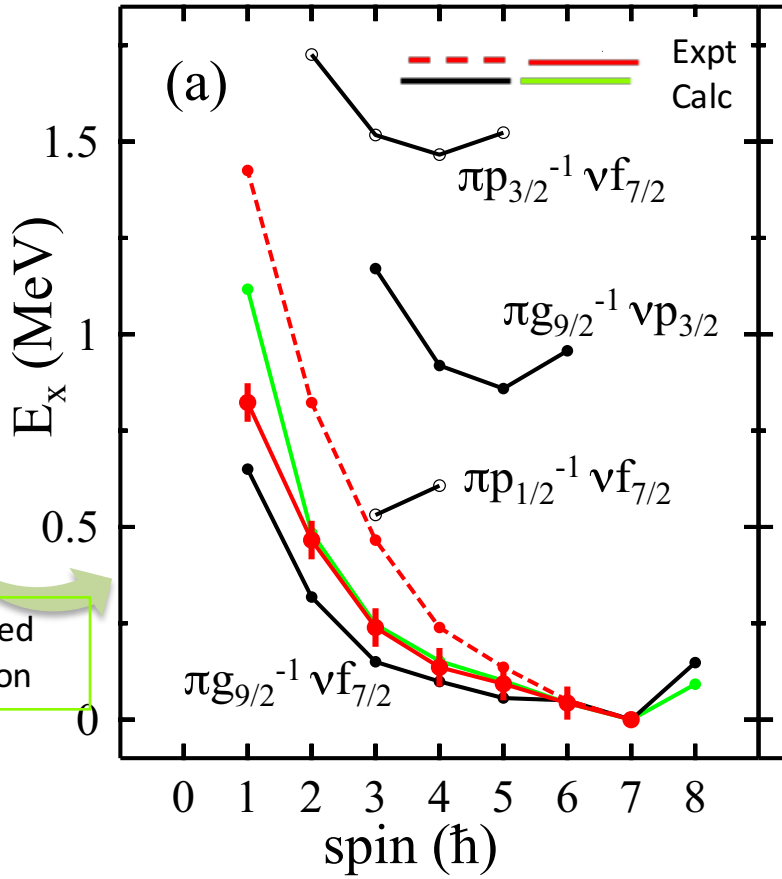

SM results with effective interaction based on a scaling of TBMEs from the ^{208}Pb region

First observation of γ rays emitted from excited states south-east of ^{132}Sn: The $\pi g_{9/2}^{-1} \otimes \nu f_{7/2}$ multiplet of ^{132}In$_{83}$

Assuming that one of the lowest transitions within the multiplet is unobserved and adopting an energy of 25 ± 25 keV for this transition

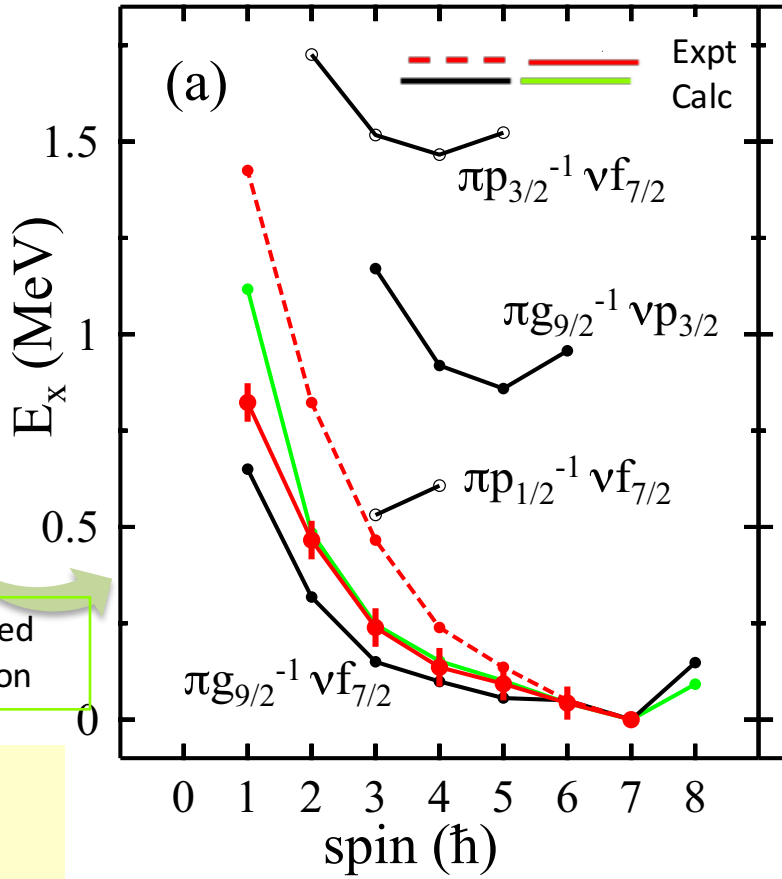

SM results with effective interaction based on a scaling of TBMEs from the ^{208}Pb region

The resulting excitation energies are much closer to the SM predictions and the average difference drops to 80 keV, i.e., 12% of the SM energy spread

PHYSICAL REVIEW C **93**, 041301(R) (2016)

First observation of γ rays emitted from excited states south-east of ^{132}Sn: The $\pi g_{9/2}^{-1} \otimes \nu f_{7/2}$ multiplet of ^{132}In$_{83}$

Assuming that one of the lowest transitions within the multiplet is unobserved and adopting an energy of 25 ± 25 keV for this transition

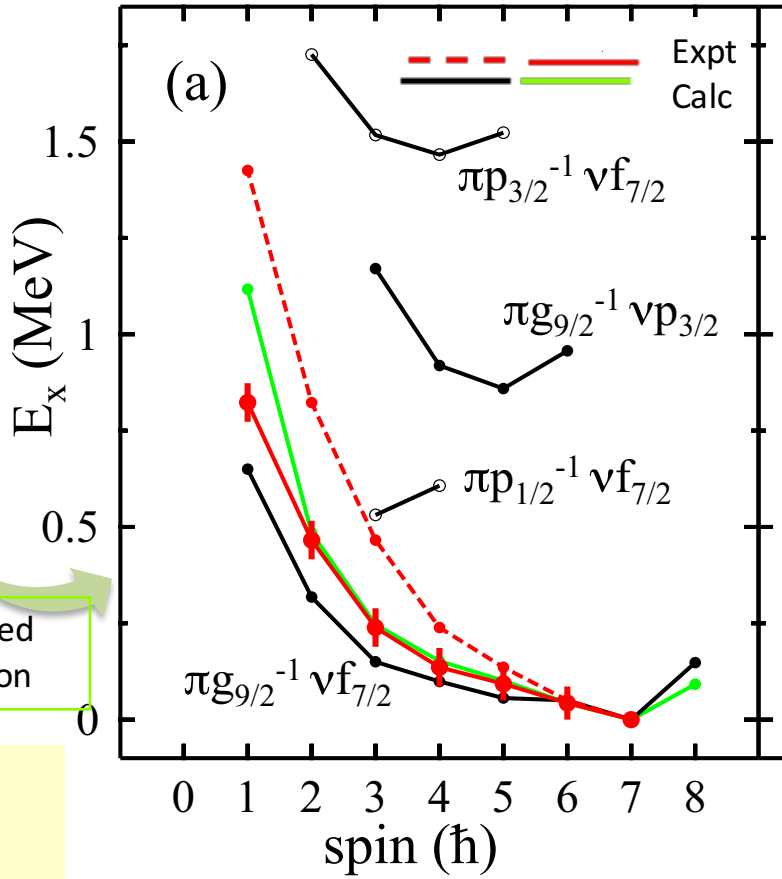

SM results with effective interaction based on a scaling of TBMEs from the ^{208}Pb region

The resulting excitation energies are much closer to the SM predictions and the average difference drops to 80 keV, i.e., 12% of the SM energy spread

More experimental information is needed!!

Conclusions

- Substantial progress has been made toward a microscopic derivation of the shell-model effective interaction
- RSMC have proved to lead to an accurate description of the structure of nuclei in ^{132}Sn regions, which makes us confident in their predictive power for physical quantities not yet measured

Conclusions

- Substantial progress has been made toward a microscopic derivation of the shell-model effective interaction
- RSMC have proved to lead to an accurate description of the structure of nuclei in ^{132}Sn regions, which makes us confident in their predictive power for physical quantities not yet measured

For a better assessment of RSMC we certainly need

✓ **more comprehensive experimental information**

✓ **to improve and extend the range of applicability of RSMC by addressing some specific questions**

Cotributors

L. Coraggio

A. Covello

A. G.

T. T. S. Kuo (SUNY, Stony Brook-USA)

N. Itaco

+ R. Liča, L. M. Fraile, A. Jungclaus,….

Thanks for your attention!